PAPER • OPEN ACCESS

Detection of spontaneous seizures in EEGs in multiple experimental mouse models of epilepsy

To cite this article: Lan Wei *et al* 2021 *J. Neural Eng.* **18** 056060

View the article online for updates and enhancements.

You may also like

- *(Invited)* Conjoint Measurement of Brain Electrophysiology and Neurochemistry
  Hitten P. Zaveri, Nimisha Ganesh, Irina I Goncharova et al.

- Intrinsic stability of ferroelectric and piezoelectric properties of epitaxial $PbZr_{0.45}Ti_{0.55}O_3$ thin films on silicon in relation to grain tilt
  Evert P Houwman, Minh D Nguyen, Matthijn Dekkers et al.

- Mouse EEG spike detection based on the adapted continuous wavelet transform
  Quang M Tieng, Irina Kharatishvili, Min Chen et al.

Journal of Neural Engineering

PAPER

Detection of spontaneous seizures in EEGs in multiple experimental mouse models of epilepsy

Lan Wei[1,2], Halima Boutouil[2,3], Rogério R Gerbatin[2,3], Omar Mamad[2,3], Mona Heiland[2,3], Cristina R Reschke[2,4], Federico Del Gallo[6,7] , Paolo F Fabene[6], David C Henshall[2,3], Madeleine Lowery[5], Gareth Morris[2,3,8] and Catherine Mooney[1,2,8,*]

1 School of Computer Science, University College Dublin, Dublin, Ireland
2 FutureNeuro SFI Research Centre, RCSI University of Medicine and Health Sciences, Dublin, Ireland
3 Department of Physiology & Medical Physics, RCSI University of Medicine and Health Sciences, Dublin, Ireland
4 School of Pharmacy and Biomolecular Sciences, RCSI University of Medicine and Health Sciences, Dublin, Ireland
5 School of Electrical & Electronic Engineering, University College Dublin, Dublin, Ireland
6 Department of Neurosciences, Biomedicine and Movement Sciences, University of Verona, Verona, Italy
7 School of Pharmacy, University of Camerino, Macerata, Italy
8 These authors contributed equally.
* Author to whom any correspondence should be addressed.

E-mail: catherine.mooney@ucd.ie

Abstract

Objective. Electroencephalography (EEG) is a key tool for non-invasive recording of brain activity and the diagnosis of epilepsy. EEG monitoring is also widely employed in rodent models to track epilepsy development and evaluate experimental therapies and interventions. Whereas automated seizure detection algorithms have been developed for clinical EEG, preclinical versions face challenges of inter-model differences and lack of EEG standardization, leaving researchers relying on time-consuming visual annotation of signals. *Approach.* In this study, a machine learning-based seizure detection approach, 'Epi-AI', which can semi-automate EEG analysis in multiple mouse models of epilepsy was developed. Twenty-six mice with a total EEG recording duration of 6451 h were used to develop and test the Epi-AI approach. EEG recordings were obtained from two mouse models of kainic acid-induced epilepsy (Models I and III), a genetic model of Dravet syndrome (Model II) and a pilocarpine mouse model of epilepsy (Model IV). The Epi-AI algorithm was compared against two threshold-based approaches for seizure detection, a local Teager-Kaiser energy operator (TKEO) approach and a global Teager-Kaiser energy operator-discrete wavelet transform (TKEO-DWT) combination approach. *Main results.* Epi-AI demonstrated a superior sensitivity, 91.4%–98.8%, and specificity, 93.1%–98.8%, in Models I–III, to both of the threshold-based approaches which performed well on individual mouse models but did not generalise well across models. The performance of the TKEO approach in Models I–III ranged from 66.9%–91.3% sensitivity and 60.8%–97.5% specificity to detect spontaneous seizures when compared with expert annotations. The sensitivity and specificity of the TKEO-DWT approach were marginally better than the TKEO approach in Models I–III at 73.2%–80.1% and 75.8%–98.1%, respectively. When tested on EEG from Model IV which was not used in developing the Epi-AI approach, Epi-AI was able to identify seizures with 76.3% sensitivity and 98.1% specificity. *Significance.* Epi-AI has the potential to provide fast, objective and reproducible semi-automated analysis of multiple types of seizure in long-duration EEG recordings in rodents.

1. Introduction

Epilepsy is a common neurological disease characterized by recurrent seizures that affects up to an estimated 70 million people worldwide [1]. Epilepsy is caused by disruption of the fine-tuned inhibitory and excitatory balance in brain networks, manifesting clinically as seizures. Electroencephalography (EEG)

is the main tool used clinically to diagnose seizures and epilepsy, and is commonly used in rodent disease models of epilepsy to study disease development, understand disease mechanisms and evaluate the effects of anticonvulsant drugs and experimental treatments. Increasingly, the field is moving toward identifying disease-modifying actions of drugs necessitating long-term recordings of EEG in rodents such as mice [2]. A key bottleneck, however, is that visual annotation of spontaneous seizures in EEG traces is time-consuming and subject to low inter-observer reproducibility and is complicated by different models and seizure types (duration, morphology). Automated seizure detection is a powerful approach to address this problem which, if sufficiently sensitive and specific, would significantly increase the throughput and reliability of seizure quantification.

One common method is to model chronic temporal lobe epilepsy (TLE) by exposure of mice to an episode of *status epilepticus* (SE) triggered by a systemic or focally-applied chemoconvulsant. Within a few days of SE, animals begin to display regular spontaneous recurrent seizures (SRS). One of the leading models uses intra-amygdala microinjection of kainic acid (IAKA) to trigger SE. This causes unilateral-onset seizures and the hallmarks of TLE [3]. It has proven highly effective as a model of epilepsy and tool for drug and biomarker discovery [4–6]. The model was originally developed in C57BL/6 mice but was later adapted to BALB/c, SJL and 129 mice. Each had modest strain-specific differences in seizure severity, convulsive behaviour or neuropathology. Another leading model of SE and subsequent SRS is the systemic administration of the muscarinic agonist pilocarpine [5, 6].

Rare genetic epileptic encephalopathies can be modelled using mice in which a disease-causing genetic mutation has been introduced. Though sharing some features of TLE, such as spontaneous seizures, the ictogenic mechanisms and electrographic characteristics of seizures in epileptic encephalopathies may have fundamental differences so it is critical to have relevant models of different epilepsy syndromes. For example, mutation of the *Scn1a* gene in mice—a model of Dravet syndrome—results in the emergence of temperature-sensitive seizures, followed by generalised tonic-clonic SRS within a few weeks [7, 8].

Very few automatic approaches to detect seizures in mouse models of epilepsy have been developed. Threshold based approaches have been applied with reported sensitivity and accuracy ranging from 90.0%–100.0% and 87.0%–94.8%, respectively [9–11]. However, the limitation of these approaches is that the results are sensitive to the threshold value and it is not clear whether thresholds apply well to different data. Machine learning approaches have the advantage that they can generalize beyond the training set [12], despite this they have only been applied to

a few mouse models of epilepsy to date. Pan *et al* [13] used weighted locally linear embedding and support vector machine based on three pilocarpine-induced SE Swiss mice to detect seizures, which achieved an accuracy between 72.8% and 90.7%. Jang *et al* [14] developed dual deep neural networks and simple pre- and post-processing on 16 non-transgenic C57BL/6 pilocarpine-induced SE mice, and tested on seven Lin28A cKO and 12 Prox1-eGFP pilocarpine-induced mice, which achieved 100.0% sensitivity and 98.0% positive predictive value. A convolutional neural network method was developed by Li *et al* [15] to detect seizures in 20 GnRH-Cre:Ai9 intrahippocampal kainic acid mice, which yielded sensitivity and specificity of 92.0% and 93.0%, respectively. However, some of these approaches detect seizures in EEG fragments rather than long-term continuous EEG recordings [9, 13], which cannot be used in a experimental setting. Additionally, they have largely used EEG recordings from a single mouse model of epilepsy. It is uncertain whether the proposed approaches would perform as well on data from other models or indeed data from the same model generated by a different researcher.

To address the limitations of earlier approaches, we sought to develop a seizure detection approach based on multiple mouse models of epilepsy. A machine learning-based seizure detection approach, Epi-AI, was utilised to detect seizures in multiple mouse models with heterogeneous seizure patterns. Epi-AI is a XGBoost-based approach, using 19 features estimated from each five-second epoch. The XGBoost classifier was implemented using nine mice for training and validation (three mouse models, Models I–III, with 20 513 s seizure and 8 258 448 s non-seizure). Furthermore, an additional 13 mice (from the three mouse models used for training, Models I–III) and four mice from a pilocarpine SE mouse model (Model IV), not used during training were used as an independent test set to further evaluate the Epi-AI approach (Model IV, with 19 566 s seizure and 14 925 934 s non-seizure). To the best of our knowledge, no methods have been developed which detect seizure events in multiple mouse models of epilepsy, making the comparison with the previous seizure detection methods in mouse models challenging. We developed two threshold-based approaches for the IAKA (mouse strain: SV129 and C57BL/6, Models I and III) and Dravet model (Model II): a local TKEO (Teager-Kaiser energy operator) and a global TKEO-DWT (Teager-Kaiser energy operator-Discrete wavelet transform) combination approach to benchmark Epi-AI. The local TKEO approach and TKEO-DWT combination approach represent standard threshold-based approaches which have been used successfully in the past to mimic how experts annotate seizures in EEGs [9–11]. These threshold-based approaches have the disadvantage that they are time-consuming to develop, and a new algorithm

Table 1. Number and duration of seizures labelled by experts (Avg: average; SZs: seizures; Dur: duration; IAKA_SV129: intra-amygdala kainic acid model of epilepsy, adult male SV129 mice; D_SV129_C57BL/6: Dravet syndrome model of epilepsy, SV129_C57BL/6 mice; IAKA_C57BL/6: intra-amygdala kainic acid model of epilepsy, adult male C57BL/6 mice; NMRI PILO: pilocarpine model of epilepsy, adult male NMRI mice).

	Model I	Model II	Model III	Model IV
Mouse strain	IAKA_SV129	D_SV129_C57BL/6	IAKA_C57BL/6	NMRI PILO
Number of mice	4	6	12	4
Number of SZs	55	12	1070	52
Avg SZs Dur(s)	38	35	34	25
SZ Dur(s)	2090	420	36 281	1288
Non-SZs Dur(s)	3997 655	1100 013	13 936 951	4149 763

must be developed for each epilepsy model with different seizure patterns as the algorithms do not generalize well between models. We show that unlike the threshold-based approach, the Epi-AI approach can be used to quantify seizures in several different mouse models of epilepsy, including one not used during training.

Epi-AI has been implemented as a publicly available web server. The user can submit an EEG file in a number of different formats (EDF, CSV, Pickle). Epi-AI returns a list of predicted seizures, including the start time, end time and duration of each, and an image of each predicted seizure. Epi-AI, and the datasets used to train and test Epi-AI, are freely available for academic users at https://lisda.ucd.ie/Epi-AI/. The Epi-AI code is available on GitHub (https://github.com/weilan0624/Epi-AI) and an executable for the local installation of Epi-AI is available on request from the authors.

2. Methods

The machine learning-based approach, Epi-AI, was developed and tested across a range of mouse models. Three mouse models of epilepsy were used to train and test Epi-AI. An additional fourth mouse model, pilocarpine SE, was used as an independent test set. Two threshold-based approaches, a local TKEO and a global TKEO-DWT combination approach, were developed to benchmark Epi-AI. The local TKEO and global TKEO-DWT represent standard threshold-based approaches that have been used successfully in the past [9–11].

2.1. Dataset

Two different mouse models of epilepsy and three different strains of mouse were used to develop the approaches in this study (Models I–III). One additional mouse model of epilepsy was used for further independent testing (Model IV) and was completely naive to training. The number and duration of seizures for each mouse model are presented in table 1. At least two experienced researchers independently identified seizures in the EEG recordings used in this study. Epochs were only labelled as seizures if they were identified as such by both

researchers. In the few cases where epochs were identified as seizure by only one researcher, they were labelled as non-seizure for the purpose of this study. Examples of the typical seizure patterns in the four mouse models are shown in figure 1.
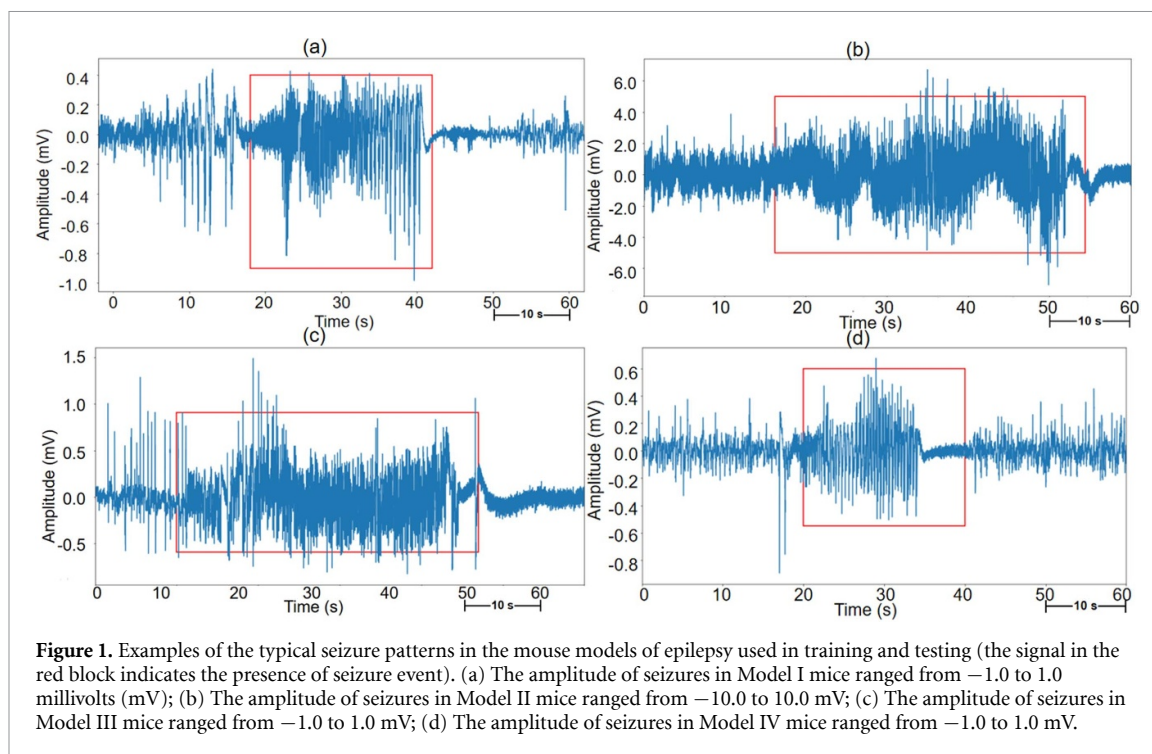
2.2. Mouse models of epilepsy

2.2.1. Intra-amygdala kainic acid model of epilepsy (Models I and III)

Procedures for inducing epilepsy using the IAKA technique in mice were approved by the Research Ethics Committee of (removed for review). Adult male 129 mice (Model I; Harlan, UK) and C57BL/6 mice (Model III; Harlan, UK) were used, based on the protocol described in [3]. For acute recordings (Model I), mice were connected to the lead socket of a swivel commutator, which was connected to an EEG (Grass TwiN digital EEG). After transmitter-cannula fitting, mice underwent intra-amygdala microinjection of kainic acid (IAKA; 0.3 μg in 0.2 μl; Sigma-Aldrich, Ireland) to induce SE followed by intraperitoneal lorazepam (8 mg kg^{-1}) after 40 min to reduce morbidity and mortality. For long term recordings (Model III), mice were anaesthetised (isoflurane; 5% induction, ~2% maintenance) and equipped for continuous EEG and video recordings using implantable EEG telemetry devices (Data Systems International, DSI). Transmitters (F20-EET for Model I and HD-X02 for Model III), which record bilateral EEG from screws embedded in the skull, were implanted in a subcutaneous pocket at the time of cannula placement (on the dura mater over the right hemisphere with the following coordinates from bregma; IA: AP = −0.95 mm, L = +2.85 mm, V = 3.1 mm). Body temperature was maintained by feedback-controlled heat blanket (Harvard Apparatus Ltd UK). Data were bandpass filtered between 0 and 500 Hz and recorded with a sampling rate of 500 Hz from mouse Models I and III. Long-term EEG was recorded for each mouse for more than 14 d.

2.2.2. Dravet syndrome model of epilepsy (Model II)

All experiments were performed in accordance with the European Communities Council Directive (86/609/EEC) and approved by the Research Ethics

Figure 1. Examples of the typical seizure patterns in the mouse models of epilepsy used in training and testing (the signal in the red block indicates the presence of seizure event). (a) The amplitude of seizures in Model I mice ranged from -1.0 to 1.0 millivolts (mV); (b) The amplitude of seizures in Model II mice ranged from -10.0 to 10.0 mV; (c) The amplitude of seizures in Model III mice ranged from -1.0 to 1.0 mV; (d) The amplitude of seizures in Model IV mice ranged from -1.0 to 1.0 mV.

Committee of (removed for review). Food and water were provided to the mice *ad libitum*. The Scn1a^{tm1Kea} targeted null allele was generated by homologous recombination in TL1 ES cells (129S6/SvEvTac) and exon 1 of the mouse *Scn1a* gene was replaced by a selection cassette as previously described [16]. Male *Scn1a*$^{(+/-)tm1Kea}$ mice on the 129S6/SvEvTac background (Jackson Laboratory, USA) were crossed with inbred female mice C57BL/6JOlaHsd (ENVIGO, UK) resulting in [129 × B6] F1.*Scn1a(+/−)* offspring, referred to herein as F1.*Scn1a*$^{(+/-)tm1Kea}$. Both male and female F1.*Scn1a*$^{(+/-)tm1Kea}$ or wild-type littermates F1.*Scn1a*$^{(+/+)tm1Kea}$ were used for experiments. At postnatal day 21 (P21) mice were placed in an adapted stereotaxic frame under anaesthesia (isoflurane/oxygen 5% for induction and ∼3% for maintenance). Body temperature was maintained by feedback-controlled heat blanket (Harvard Apparatus Ltd UK). Following a midline scalp incision, three screw electrodes were implanted, and the unit was secured with dental cement. The screw electrodes were placed bilaterally about the midline over the cerebral cortex, and the reference electrode positioned over the nasal sinus. After surgery, animals were immediately placed in an incubator at 33 °C and monitored. Once fully recovered, mice were connected to the lead socket of a swivel commutator, which was connected to an EEG amplifier (Xltek, 32 channels, Natus Neurology, WI, USA). EEG data were recorded from 12:30 pm to 6:30 pm each day from P21 to P28. Data were bandpass filtered between 0 and 512 Hz and recorded with a sampling rate of 512 Hz from mouse Model II. Two of the six mice used were additionally treated with an experimental
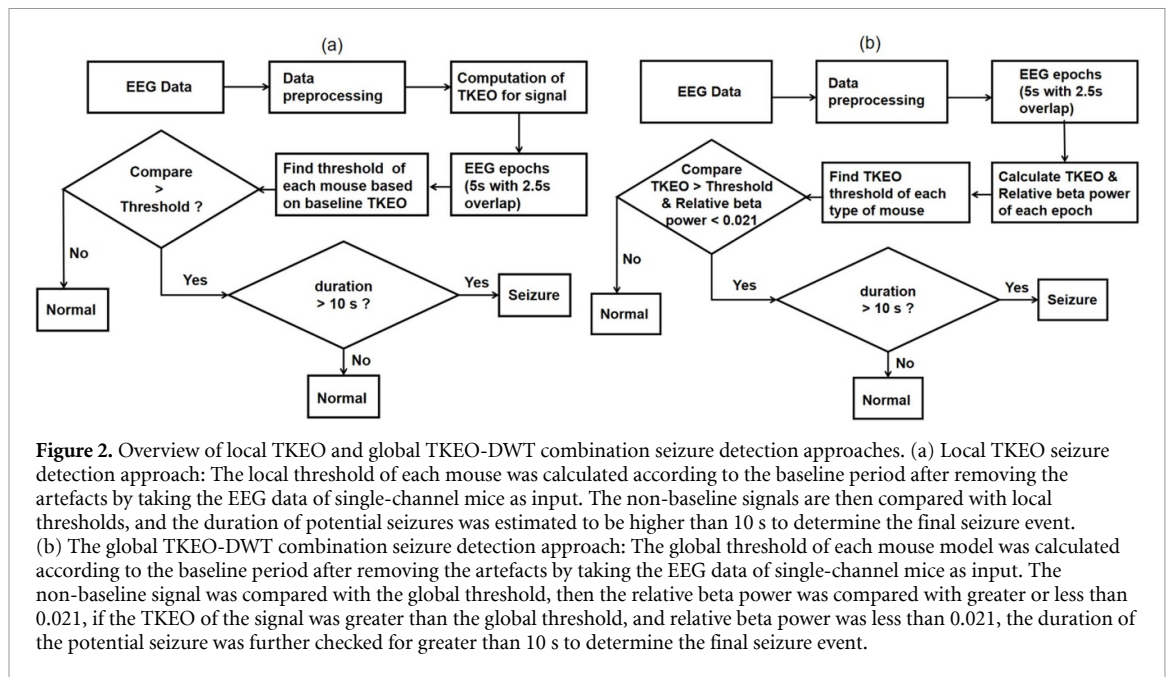
antisense oligonucleotide, but this had no effect on any seizure, electrographic or other parameters in the model.

2.2.3. Pilocarpine model of epilepsy (Model IV)
The pilocarpine model of TLE was performed as previously described [17]. Adult male NMRI mice were fitted for DSI telemetry as above. Briefly they were anesthetised (isoflurane 5% induction followed by 2% maintenance) and equipped with the DSI F20-EET telemetry device. During surgery, transmitters were implanted into a subcutaneous pocket at the level of the peritoneum. Leads run subcutaneously to the head of the animal, two to the right nuchal muscle which serve as EMG electrodes. The other two were implanted to the surface of the dura mater via a small craniotomy with the following coordinates relative to Bregma, AP: $+1.7$, L: -1.5 and AP: -2.5, L: $+2.0$ mm. Following surgery, animals were placed in Phenotyper® cages (Noldus Information Technologies®, Wageningen, the Netherlands) to recover. Following recovery, animals were given methylscopolamine (1 mg kg^{-1}) to block peripheral cholinergic actions and then after 30 min, injected with pilocarpine IP (300 mg kg^{-1}) and the development of SE and SRS was recorded [6]. Data were bandpass filtered between 0 and 500 Hz and recorded with a sampling rate of 500 Hz from mouse Model IV. The EEG recording time of each mouse was no less than 3 d and up to 26 d.

2.3. Data analysis
EEG signals from mouse Model II were resampled from 512 Hz to 500 Hz, for consistency with the other

Figure 2. Overview of local TKEO and global TKEO-DWT combination seizure detection approaches. (a) Local TKEO seizure detection approach: The local threshold of each mouse was calculated according to the baseline period after removing the artefacts by taking the EEG data of single-channel mice as input. The non-baseline signals are then compared with local thresholds, and the duration of potential seizures was estimated to be higher than 10 s to determine the final seizure event. (b) The global TKEO-DWT combination seizure detection approach: The global threshold of each mouse model was calculated according to the baseline period after removing the artefacts by taking the EEG data of single-channel mice as input. The non-baseline signal was compared with the global threshold, then the relative beta power was compared with greater or less than 0.021, if the TKEO of the signal was greater than the global threshold, and relative beta power was less than 0.021, the duration of the potential seizure was further checked for greater than 10 s to determine the final seizure event.

EEG recordings. A 50 Hz notch filter was applied to remove the 50 Hz power line interference from the EEG recordings, the DC offset was also removed. The EEG signal was divided into 5 s epochs with 2.5 s overlap. Signal features were then estimated for each epoch as described below.

2.4. Threshold-based seizure detection approaches
Two threshold-based seizure detection approaches were developed to act as a benchmark for the machine learning-based approach. The local TKEO approach detects seizure events in long EEG recording in mouse Model I by checking the amplitude, frequency range, and signal power which mimics how experts detect seizures in mouse Model I. The global TKEO-DWT combination approach analyses the signal in both time and frequency domains in three mouse models of epilepsy (Models I–III).

2.4.1. Local TKEO approach
A TKEO was applied to distinguish the seizure from the non-seizure EEG signal. Due to the simplicity and ease of implementation of TKEO, it has been shown to be powerful in identifying changes in signal properties in applications such as speech processing [18], seizure detection [19, 20] and the onset of muscle activity in electromyography (EMG) recordings [21]. This approach mimics how experts detect seizure during the EEG recordings by examining changes in signal amplitude. The TKEO value in each epoch was defined as:

$$\text{TKEO}[n] = x[n]^2 - x[n-1]x[n+1] \quad (1)$$

where $x[n]$ is the nth sample, $x[n-1]$ is the $(n-1)$th sample and $x[n+1]$ is the $(n+1)$th sample of the pre-processed EEG signal in the epoch.

The threshold was defined as the twice the mean TKEO value of the baseline EEG (first 20 min) of each mouse. The TKEO of each five-second epoch from the non-baseline (EEG signal from 20 min to the end of the EEG recordings) period was then compared with the threshold. If the TKEO value in the epoch was greater than the threshold, the event was labelled as a potential seizure. The duration of the potential seizure was checked, and if the duration of the event was greater than 10 s it was defined as a seizure, if not, it was labelled as a regular event (figure 2(a)). Figure 6 shows the local TKEO approach applied to a representative EEG signal.

2.4.2. Global TKEO-DWT combination approach
The discrete wavelet transform (DWT) has been successfully used in EEG seizure detection [22–24]. In this study, DWT with a function Daubechies 4 wavelet (db4) was used, as the smoothness of db4 wavelet makes it more suitable for detecting changes of EEG signals [25]. The DWT has near-optimal time-frequency localization [26] and was used to decompose the EEG signal into seven different frequency bands, corresponding to different brain rhythms [27]. The signals were separated into the delta (A7), theta (D7), alpha (D6), beta (D5), gamma (D4), high gamma (D3), ripple (D2), and fast ripple (D1) [28] as defined in table 2.

A global TKEO-DWT combination approach to seizure detection was developed based on the TKEO approach and DWT. This approach analyses the signal in both time and frequency domains. The global TKEO threshold was defined as the mean value of the local TKEO threshold for each mouse Models I–III. A second threshold based on the DWT was then calculated by estimating the mean value of relative beta

Table 2. Seven level of wavelet decomposition.

Decompose level	Frequency range (Hz)	Signal information
D1	250–500	Fast ripple
D2	125–250	Ripple
D3	63–125	High gamma
D4	32–63	Gamma
D5	16–32	Beta
D6	8–16	Alpha
D7	4–8	Theta
A7	0–4	Delta

power (the ratio of the power in the D7 beta band relative to the total power in the signal from 0 to 500 Hz) in each epoch from mouse Models I–III. From table 3 we can see that if the relative beta power was smaller than 0.021 in each epoch it was more likely to be a seizure event. Therefore, we defined the DWT threshold as relative beta power smaller than 0.021. For the global TKEO-DWT combination approach, first, the mean TKEO value of a non-baseline epoch was compared with the global threshold, if the TKEO value was greater than the global threshold, the relative beta power in that epoch was then checked to see if it was less than 0.021. If the mean TKEO value of the epoch was greater than the global TKEO threshold and the relative beta power in that epoch was less than 0.021, the epoch was defined as a potential seizure event. Otherwise, the epoch will be defined as a non-seizure event. Furthermore, the duration of the potential seizure event was further checked. If the duration of the potential seizure event lasts longer than 10 s, it was defined as a final seizure event. Otherwise, the event was finally labelled as a non-seizure event. Figure 2 (b) presents the structure of the global TKEO-DWT combination approach.

2.5. XGBoost-based seizure detection approach: Epi-AI

Nineteen features were estimated to develop the XGBoost algorithm, including a selection of time and frequency domain features previously used in seizure detection [29–32], and features used in manual seizure detection from EEG in these mouse models of epilepsy. All features were estimated for each 5 s epoch. Next, each epoch was predicted to a seizure or non-seizure event by the XGBoost algorithm. The duration of seizures is typically defined as at least 10 s [33], a filter was used to check if the duration of the potential seizure event detected by the algorithm was greater than 10 s or not. If higher than 10 s, the potential seizure event was defined as a seizure event. Otherwise, it was labelled as a non-seizure event. Then we post-processed the detect seizure events to define the start and end of the seizure. An overview of Epi-AI is presented in figure 3.

2.5.1. Feature estimation

Nineteen time and frequency domain features were estimated for each 5 s epoch for each EEG signal from Models I to III. The estimated features are: (a) mean value of TKEO; the absolute power of the (b) delta (0–4 Hz), (c) theta (4–8 Hz), (d) alpha (8–16 Hz), (e) beta (16–32 Hz), and (f) gamma (32–64 Hz) frequency bands; the relative power of the (g) delta, (i) theta, (j) alpha, (k) beta, and (l) gamma frequency bands; (m) total absolute power (0–500 Hz); (n) mobility; (o) mean; (p) variance; (q) kurtosis; (r) skewness; (s) mean of the envelope (estimated using the Hilbert transform) and (t) fractal dimension (FD) of the pre-processed signal. The mobility and FD were estimated as:

$$FD = \frac{\log_{10}^{N}}{\log_{10}^{N} + \log_{10}^{N/(N+0.4\delta))}} \qquad (2)$$

$$Mobility = \sqrt{\frac{Var(\dot{x})}{Var(x)}} \qquad (3)$$
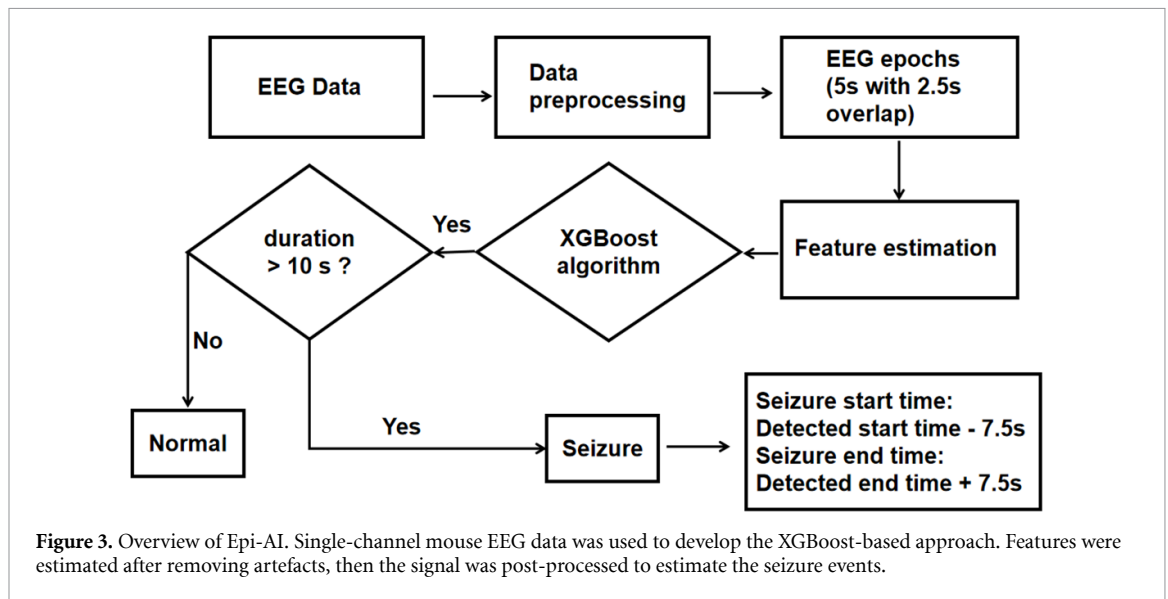
where N is the number of samples in each epoch; and δ is the number of sign changes in the signal derivative in that epoch; $\dot{x}$ is the time derivative of the pre-processed EEG signal x, and Var (x) is the variance of x estimated for that epoch.

2.5.2. Predictive architecture

The XGBoost algorithm is widely used to achieve state-of-the-art results on many machine learning challenges [34] and especially has been widely used to detect seizures in human EEG recordings [35–37]. Moreover, it is generic enough to be applied to large-scale problems, runs more than ten times faster than existing popular solutions on a single machine, and returns a measure of feature importance [34] (figure 4). Furthermore, as the seizure events in the dataset were much fewer than non-seizure events, resulting in a class imbalance problem that can make training a machine learning algorithm challenging [38], parameter 'scale pos weight' in XGBoost classifier can be adjusted to balance the events in the training set. In preliminary work, four other algorithms (naive bayes, K nearest neighbours, decision tree and random forest) were benchmarked against the XGBoost classifier. The XGBoost algorithm achieved higher receiver operating characteristics curve (AUROC) and was chosen for this study (see table A1). The XGBoost was implemented within the Python 3 environment. Four parameters were optimized: learning-rate: shrinks the contribution of each tree; n-estimators: the number of boosting stages to perform; max-depth: the maximum depth of the individual regression estimators; scale-pos-weight: balancing of positive and negative weights.

Table 3. Relative beta power in seizure and non-seizure event (RBP: relative beta power; std: standard deviation; Avg: average).

Model	Event	Mean of RBP	Std of RBP	Mean+std	Mean−std
I	Seizure	0.003	0.006	0.009	−0.003
	Non-seizure	0.025	0.018	0.043	0.007
II	Seizure	0.005	0.007	0.012	−0.002
	Non-seizure	0.032	0.006	0.039	0.026
III	Seizure	0.026	0.024	0.050	0.002
	Non-seizure	0.032	0.008	0.040	0.024
*Avg	**Seizure**	0.011	0.008	**0.020**	0.003
	Non-seizure	0.028	0.005	0.033	**0.022**

Figure 3. Overview of Epi-AI. Single-channel mouse EEG data was used to develop the XGBoost-based approach. Features were estimated after removing artefacts, then the signal was post-processed to estimate the seizure events.

2.5.3. Training and testing

Nine mice were used for training and validation, and the other 17 mice were used as an independent test set. The allocation to the training/validation or independent test sets depended on the duration of the seizures in each mouse. Mice were allocated to either the training/validation or independent test sets so that sum of the seizure duration was approximately equal between the sets for each mouse model and between the training/validation or independent test sets, i.e. the total seizure duration from mouse Models I–III in the training/validation set is 20 513 s, and 18 278 s in the independent test set. The training and validation sets were split so that 80% was used for training and 20% for validation. The duration of seizure/non-seizure used in the training/validation and the independent test sets are shown in table 4. The independent test set was not used in training. Specifically, no mice of type Model IV was used in training the models, therefore the models are completely naive to mice of this type. Four parameters (learning-rate, n-estimators, max-depth, and scale-pos-weight) were optimized based on the performance of the validation set. The best performance on the validation set was achieved when learning-rate = 0.01, n-estimators = 100, max-depth = 6 and scale-pos-weight = 478.

2.5.4. Post-processing: seizure estimation

EEG typically contains artefacts which may interrupt and mask the seizure trace [39]. To overcome this, the seizures detected by the XGBoost algorithm with an interval less than 5 s were grouped together, and their duration was extended from the start time of the first component to the end time of the last component. As the duration of seizure in the experimental mouse models of epilepsy is typically longer than 10 s, the potential seizures detected by the method with duration less than 10 s were relabelled as non-seizure events (figure 3). Since the start time and the end time of the seizure events are difficult to define and identify, in order not to miss seizure events, if the duration of the potential seizure detected by the method was greater than 10 s and the final seizure start time was 7.5 s ahead of the detected potential seizure start time, the final seizure end time was extended 7.5 s backward to the detected potential seizure end time (figure 5).

2.5.5. Implementation

The Epi-AI approach was implemented in Python 3.6.5 (MSC v.1900 64 bit (AMD64)) and IPython 6.4.0 in Jupyter notebook v. 4.4.0 from Anaconda. The approach was run on a Windows 10 desktop with Intel(R) Core(TM) i7-7700HQ CPU (4 cores).
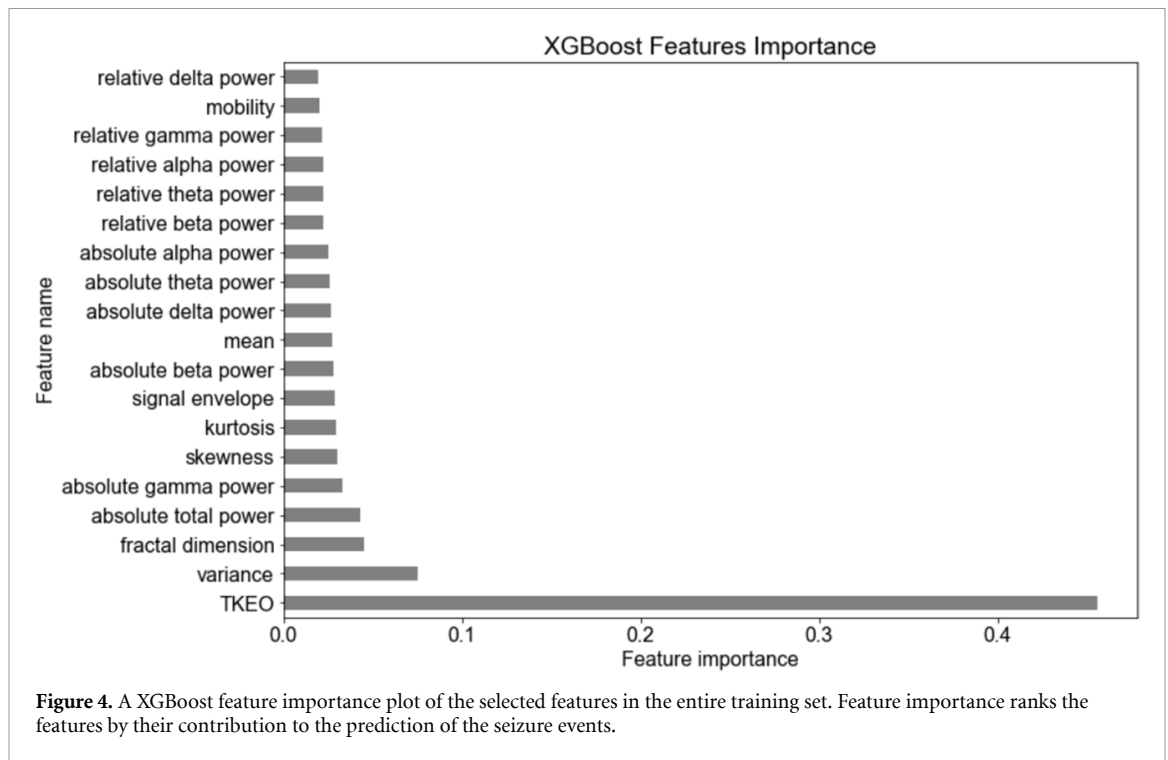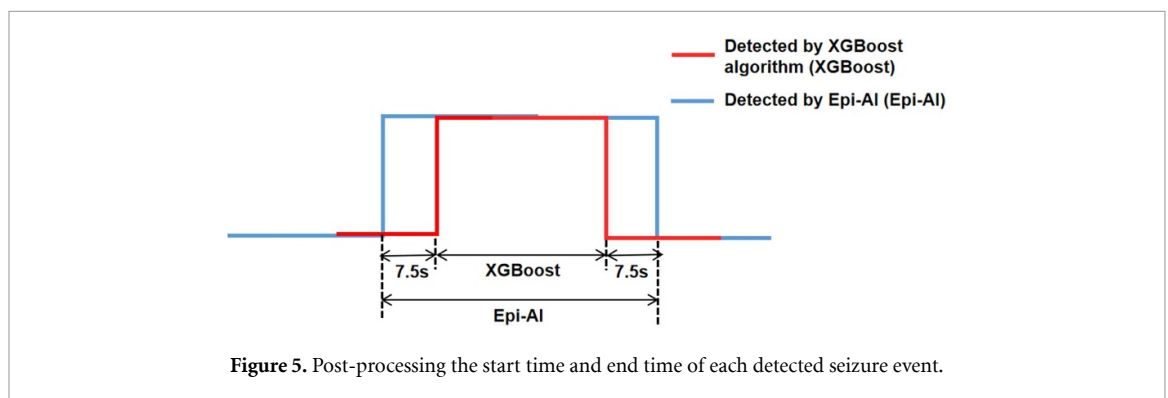
Figure 4. A XGBoost feature importance plot of the selected features in the entire training set. Feature importance ranks the features by their contribution to the prediction of the seizure events.

Table 4. The number of mice and the duration of seizures allocated to the training/validation set and the independent test set for the XGBoost-based approach.

	Model	Number of mice	Seizure duration(s)	Non-seizure duration(s)
Training/ validation set	I	1	990	1094 197
	II	2	300	308 293
	III	6	19 223	6855 958
	Total	**9**	**20 513**	**8258 448**
Independent test set	I	3	1100	2903 458
	II	4	120	791 720
	III	6	17 058	7080 993
	IV	4	1288	4149 763
	Total	**17**	**19 566**	**14 925 934**

Figure 5. Post-processing the start time and end time of each detected seizure event.

It took approximately 15 s to analyse 3600 s data. Epi-AI has also been implemented as a web server (https://lisda.ucd.ie/Epi-AI/) which allows users to upload single-channel EEG data and returns the start and end times of detected seizure events along with the corresponding spectrograms. Representative traces (one hour duration) are also available for each model (Models I–IV) used in this study for download through the web server along with sample code.

2.6. Evaluation metrics

The area under the receiver operating characteristics curve (AUROC) was used to estimate the

performance of Epi-AI, along with the accuracy (Acc), sensitivity (Sens), and specificity (Spec).

$$Acc = \frac{TP + TN}{TP + TN + FP + FN} \qquad (4)$$

$$Sens = \frac{TP}{TP + FN} \qquad (5)$$

$$Spec = \frac{TN}{TN + FP} \qquad (6)$$

where true positives (TP) is the number of epochs predicted as seizures that were also identified as seizures by the expert readers; false positives (FP) is the number of epochs predicted to be seizures that were identified as non-seizures by the expert readers; true negatives (TN) is the number of epochs predicted to be non-seizures that were identified as non-seizures by the expert readers; false negatives (FN) is the number of epochs predicted to be non-seizures that were identified as seizures by the expert readers.

3. Results

Table 5 compares the performance of the Epi-AI against the local TKEO, global TKEO-DWT combination approach on the independent test set across all mouse models (Models I–V). The local TKEO approach was developed to mimic the researchers' examination of seizure events in mouse Model I, with a sensitivity of 72.1% and a specificity of 97.5% on mouse Model I. However, when the local TKEO approach was applied to mouse Models II and III the sensitivity and specificity was only 66.9%–91.3% and 60.8%–69.9% respectively. On the independent test set, mouse Model IV, the sensitivity was further reduced to 55.2%. Figure 6 presents an example of the local TKEO approach applied to a representative EEG signal. The global TKEO-DWT combination approach detected seizures in mouse Models I–III at 73.2%–80.1% sensitivity, 75.8%–98.1% specificity and 75.8%–98.1% accuracy. On the independent test set, the global TKEO-DWT combination approach achieved sensitivity, specificity and accuracy of 37.7%, 98.5% and 98.4%, respectively on the mouse Model IV. Figure 7 presents the global TKEO threshold applied to a representative EEG signal.

Epi-AI obtained a sensitivity of 91.4%–98.8%, a specificity of 93.1%–98.8% and accuracy of 93.1%–98.8% on the independent test set of mouse models which were used for training (Models I–III) when compared with expert human annotations. When tested on an independent test set, Model IV, which was not used to train the approach, the Epi-AI algorithm achieved 76.3% sensitivity, 98.1% specificity and 98.1% accuracy.
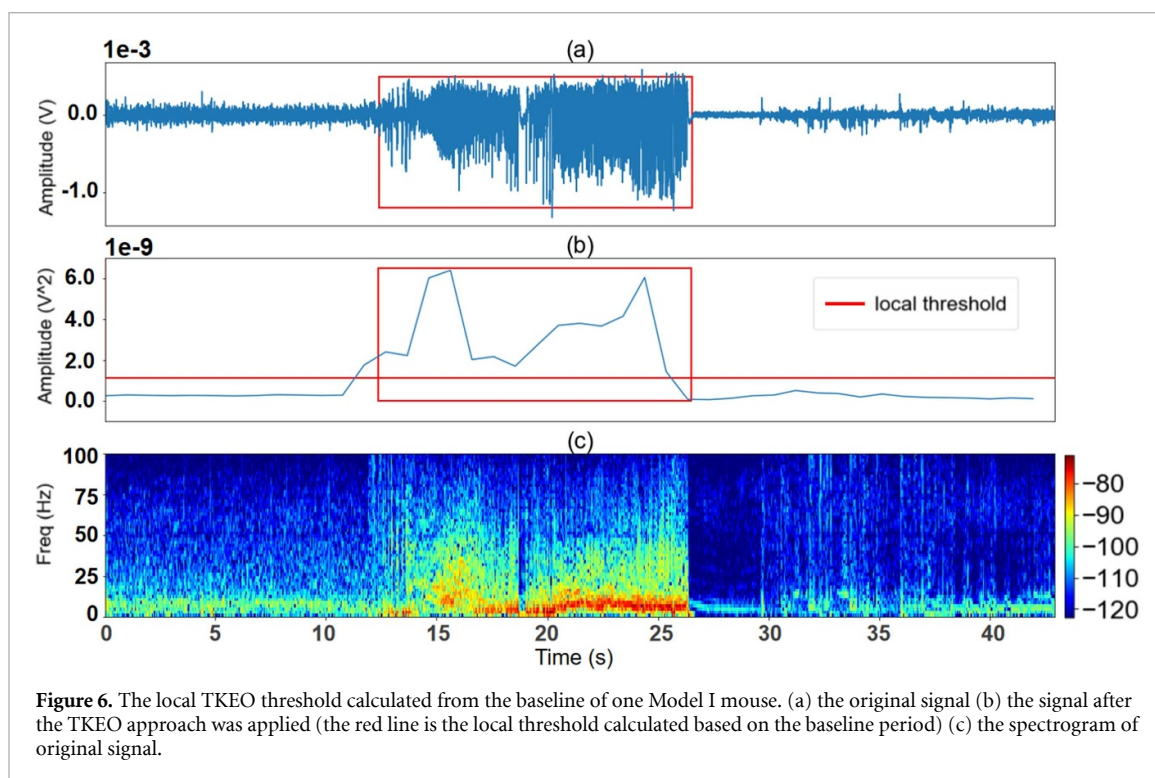
4. Discussion

The lack of reliable automated seizure detection approaches is a major impediment to the study of epilepsy development and testing of experimental treatments in rodents. We have developed an XGBoost-based algorithm, Epi-AI, that can generalise to multiple mouse models of both genetic and acquired epilepsies (Models I–III, with sensitivity 91.4%–98.8% on the mouse models used in training), including one not used in the training of the algorithm (Model IV, with sensitivity 76.3%). Previous studies have used only a single model on which to develop a detection approach [9, 11, 13–15, 40], limiting the translation and generalisation of techniques between models or individual users.

A key advantage of the Epi-AI approach is the combination of multiple different mouse models of epilepsy, with differing underlying epileptogenic mechanisms. To the best of our knowledge, none of the previously developed approaches [9, 11, 13–15, 40] have demonstrated that they can detect seizures in multiple mouse models of epilepsy in continuous EEG recordings (table 6). In previous studies, Pan *et al* [13], Jang *et al* [14] and Li *et al* [15] used machine learning approaches to detect seizure events in single mouse models of epilepsy, achieving 76.4% to 99.3% accuracy. Tieng *et al* [11] proposed a new seizure detection approach based on multiple features and a simple thresholding technique on pilocarpine mouse model which achieved 100% sensitivity and 72% specificity. However, these approaches are limited to the training model. Epi-AI can detect seizures not only for the mouse models used in training (Models I–III), but also for the independent test set (mouse Model IV) (table 5). The training models included an intra-amygdala kainic acid model of acquired TLE and a genetic model of Dravet syndrome, whilst the independent test set used the pilocarpine model of TLE. This indicates that Epi-AI can generalise to detect electrographic seizures with entirely different pathological mechanisms while also being able to detect seizures based on electrographic signatures which are common between models. Epi-AI could therefore also be applied to seizure detection in other models or studies where limited dataset sizes may not permit the development of a dedicated algorithm for that model.

The difference in datasets and means of evaluating performance make a direct comparison with other published seizure detection approaches difficult [41]. We developed the local TKEO approach and TKEO-DWT combination approach as a benchmark to represent standard threshold-based approaches that have been used successfully in the past [9–11]. The local TKEO approach mimics how experts detect seizures in mouse Model I by checking the amplitude, frequency range, and signal power. TKEO can determine the instantaneous energy of the non-stationary

Table 5. The performance of the threshold-based approaches (local TKEO approach and global TKEO-DWT combination approach), and the performance of Epi-AI on the independent test set of four mouse models of epilepsy.

	Model	Acc($\pm$std)(%)	Sens($\pm$std)(%)	Spec($\pm$std)(%)	AUROC($\pm$std)
Local TKEO	I ($n = 3$)	98.0($\pm$ 0.7)	72.1($\pm$12.0)	97.5($\pm$ 0.1)	0.923($\pm$0.086)
	II ($n = 4$)	69.9($\pm$23.3)	66.9($\pm$23.6)	69.9($\pm$23.3)	0.737($\pm$0.060)
	III ($n = 6$)	60.9($\pm$37.3)	91.3($\pm$ 8.0)	60.8($\pm$37.5)	0.753($\pm$0.176)
	IV ($n = 4$)	97.2($\pm$ 2.3)	55.2($\pm$35.8)	97.2($\pm$ 2.3)	0.683($\pm$0.133)
Global TKEO-DWT	I ($n = 3$)	98.1($\pm$ 2.2)	80.1($\pm$30.2)	98.1($\pm$ 2.2)	0.891($\pm$0.152)
	II ($n = 4$)	75.8($\pm$18.2)	79.2($\pm$21.7)	75.8($\pm$18.2)	0.775($\pm$0.050)
	III ($n = 6$)	82.9($\pm$18.4)	73.2($\pm$15.1)	82.9($\pm$18.5)	0.781($\pm$0.102)
	IV ($n = 4$)	98.4($\pm$ 1.3)	37.7($\pm$ 8.9)	98.5($\pm$ 1.3)	0.681($\pm$0.043)
Epi-AI	I ($n = 3$)	98.8($\pm$ 1.6)	91.4($\pm$24.4)	98.8($\pm$ 1.6)	0.952($\pm$0.117)
	II ($n = 4$)	97.2($\pm$ 2.1)	98.8($\pm$ 2.4)	97.2($\pm$ 2.1)	0.980($\pm$0.018)
	III ($n = 6$)	93.1($\pm$13.0)	96.4($\pm$ 7.0)	93.1($\pm$13.1)	0.947($\pm$0.067)
	IV ($n = 4$)	98.1($\pm$ 3.0)	76.3($\pm$24.0)	98.1($\pm$ 2.9)	0.873($\pm$0.129)

Figure 6. The local TKEO threshold calculated from the baseline of one Model I mouse. (a) the original signal (b) the signal after the TKEO approach was applied (the red line is the local threshold calculated based on the baseline period) (c) the spectrogram of original signal.

signal. In addition to energy, TKEO can also track instantaneous amplitude, and frequency of a signal [42], widely used in events detection in biomedical signals. As the TKEO approach mimics how experts detect seizures in mouse Model I, this approach performs well on mouse Model I (table 5). Moreover, the TKEO approach is easily understood by experts and is easy to interpret and reproduce. However, it does not generalise well to mouse Models II, III and IV.

The global TKEO-DWT combination approach analyse the signal in both time and frequency domains, which generalises well on the three mouse models used in training (Models I, II, and III), which demonstrated that the global TKEO-DWT combination approach could be used to detect seizure events in intra-amygdala kainic acid (IAKA_SV129 and IAKA_C57BL/6) and Dravet syndrome (D_SV129_C57BL/6) model of epilepsy

(table 5). In addition, the global TKEO-DWT combination approach can also be adjusted to fit the seizure type of the different mouse models for better accuracy. However, the global TKEO-DWT combination approach did not perform well on the independent test set (Model IV), which was entirely naive of training, only achieving a sensitivity of 37.7%.

Because of the large number of false-positive events, Epi-AI provides a visualisation of the detected seizure events to assist users to filter out these false-positive events manually by checking the amplitude and the spectrogram of the detected events. As Epi-AI is trained on manual annotation of experts, the predictions can not be superior to experts, however, after training, Epi-AI will always assign similar annotations to the seizure events, enabling a more objective detection of seizure events in EEG recordings thereby reducing the current variability among experts due
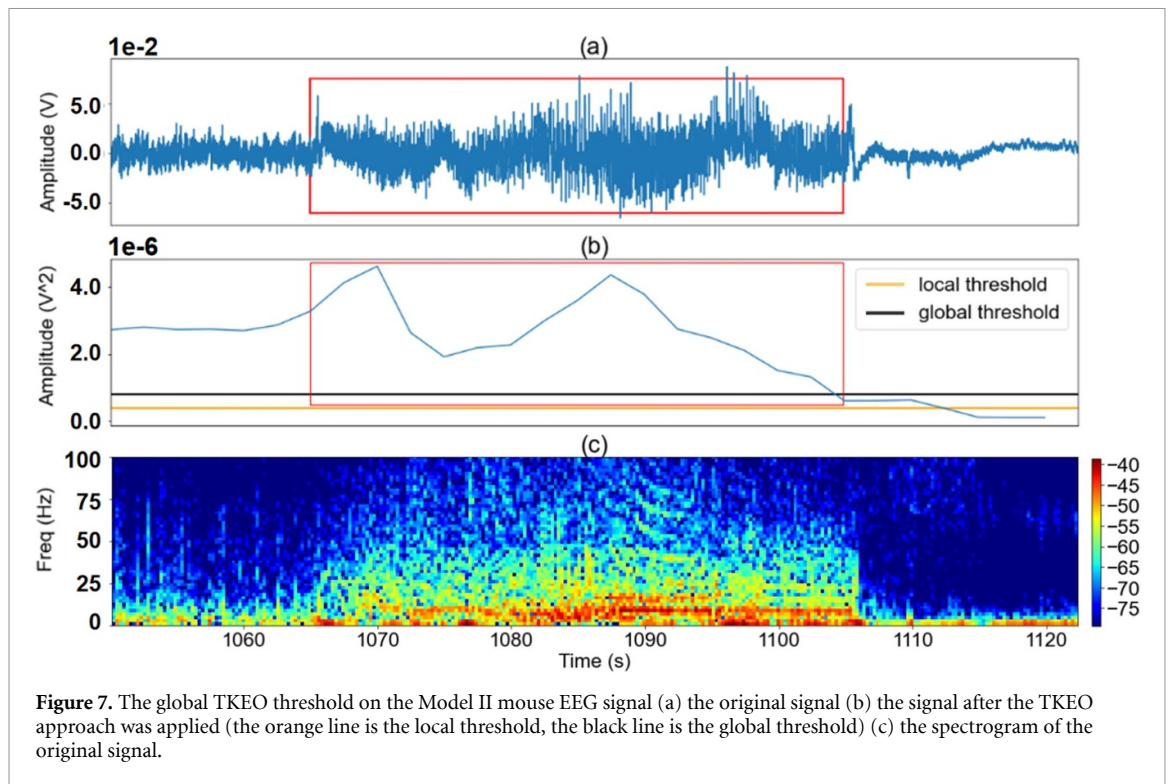
Figure 7. The global TKEO threshold on the Model II mouse EEG signal (a) the original signal (b) the signal after the TKEO approach was applied (the orange line is the local threshold, the black line is the global threshold) (c) the spectrogram of the original signal.

Table 6. The performance of Epi-AI on the independent test set of four mouse model of epilepsy and other proposed work (*N*: number of subjects; Dur: duration of EEG recordings; IAKA: intra-amygdala microinjection of kainic acid; DS: Dravet syndrome; GA: genetic absence seizure model; PL: pilocarpine-induced SE model; IHKA: intrahippocampal kainic acid).

Reference	Strain	Model	N	Dur (*h*)	Acc (%)	Sens (%)	Spec (%)
[40]	Male WAG/Rij rat	GA	6	—	94.8	—	—
[9]	F344 rats	GA	4	8.0	> 90.0	> 90.0	—
[11]	Outbred CD1 mice	PL	12	2016.0	—	100.0	72.0
[13]	Male Swiss mice	PL	1	0.2	76.4	—	23.6
[14]	Lin28A cKO&Prox1-eGFP mice	PL	19	4272.0	—	100.0	—
[15]	GnRH-Cre:Ai9 mice	IHKA	20	10.6	93.0	92.0	93.0
Epi-AI	Male SV129	IAKA	3	806.8	98.8	91.4	98.8
	SV129C57BL/6	DS	4	220.0	97.2	98.8	97.2
	Male C57BL/6	IAKA	6	1971.7	93.1	96.4	93.1
	NMRI	PL	4	1153.1	98.1	76.3	98.1

to human errors, human preferences, label environments, or the level of vigilance [43].

Another advantage of our approach is that Epi-AI can provide the relative importance of features used to train the algorithm. This revealed that the TKEO is the most critical feature in the Epi-AI approach (figure 4). In applications such as speech processing [18] and seizure detection [19, 20], TKEO has shown strong function in recognizing changes in signal properties. The local TKEO approach proposed in this study also achieved high accuracy in the detection of seizure events in mouse Model I. This finding suggests that TKEO could represent a key common electrographic feature of seizure activity in multiple types of epilepsy. However, our results demonstrate that seizure detection using TKEO alone does not generalise well between models, and therefore the other features used by Epi-AI, whilst individually less

relevant, combine to form a more generalisable model of seizure detection.

A final advantage is that we estimated EEG features for Epi-AI from 5 s epochs, with 2.5 s overlap. The selection of a smaller epoch (5 s) is more computationally expensive but allows us to more accurately define the start and end of seizure events. We defined the minimum seizure duration to be 10 s [33]. The epoch size therefore must be shorter than the minimum seizure duration, to avoid the inevitable inclusion of non-seizure periods within epochs labelled as seizures, and to facilitate a more accurate readout of seizure timing. In contrast, other studies divided EEG traces into longer epochs (for example 23.6 s in [44]) for feature estimation. If applied to our seizure definitions, we could hypothetically label an entire 23.6 s epoch as seizure activity, whereas it may in fact be composed of 10 s seizure activity and 13.6 s

non-seizure activity. Therefore, by using a smaller epoch size, we can more reliably determine seizure onset and termination.

A main limitation of this work is that the Epi-AI did not perform as well on mouse Model IV, which was not part of the training set, compared to the other three mouse models (Models I–III). It is probable that Epi-AI learned characteristics of the seizure events that are specific to Models I–III that do not generalise to mouse Model IV. However, sensitivity and specificity greater than 75% and 95% respectively on Model IV suggests that Epi-AI can still generalise to a reasonable extent. Another limitation of this work is that the 'gold standard' is also subject to variability or errors, as expert human reviewers do not always agree. Some studies examined the kappa scores of seizure annotation by two to eight experts, with kappa score ranging from 0.49 to 0.85 [45–47]. However, in order to make the annotation more convincing, in this study, the EEGs were annotated by seven experts as the 'gold standard' (at least two experts cross-scored/validated the annotations of each dataset).

Overall, manual identification of seizure events in EEG recordings by experts is time consuming and subject to inter-rater variability. The advantage of Epi-AI over manual scoring is that the seizure events in each mouse EEG recording could be estimated in less than a minute, whereas manually annotation by experienced experts could take hours. As machine learning is a 'black box' method, users may have difficulty trusting machine learning-based methods [48]. We have implemented Epi-AI as a web server, which allows users to more easily and quickly explore seizures events. The visualisation of the amplitude and corresponding spectrogram of each predicted seizure event provided by the Epi-AI web server will allow the user to quickly filter out false positives manually, which will help to gain the user's trust in the system and improve overall accuracy. We believe that this will enhance the potential for Epi-AI to be used more widely in epilepsy research.

5. Conclusion

In this paper, we describe a novel XGBoost-based approach, Epi-AI, to detect seizures in EEG recordings in multiple mouse models of epilepsy.

We benchmarked Epi-AI against a local TKEO and a global TKEO-DWT combination approach which represent standard threshold-based approaches. Epi-AI demonstrated sensitivity of 76.3% to 98.8%, and specificity of 93.1% to 98.8% on the independent test set. We show that Epi-AI generalizes well to several different mouse models, including one not used in the development of the approach. Epi-AI represents a powerful new approach to automated unbiased seizure detection from EEG data in multiple rodent epilepsy models on single channel EEG. Moreover, Epi-AI has been implemented as a web server, allowing users to submit a single-channel EEG file, which will be annotated by Epi-AI and returned to the user in a matter of seconds. Therefore, Epi-AI has the potential to be beneficial in research by greatly improving the speed, reliability and reproducibility of seizure analysis in rodent EEG data.

Data availability statement

The data that support the findings of this study are openly available at the following URL/DOI: https://lisda.ucd.ie/Epi-AI/.

Appendix. Preliminary analysis

Figure A1 presents the local TKEO, global TKEO-DWT combination, and Epi-AI approaches applied on Model I–IV EEG signal.

Table A1. Preliminary analysis (without post-processing) of the performance of the XGBoost algorithm for seizure detection compared to four other algorithms on the validation set (NB: naive bayes; KNN: K nearest neighbors; DT: decision tree; RF: random forest).

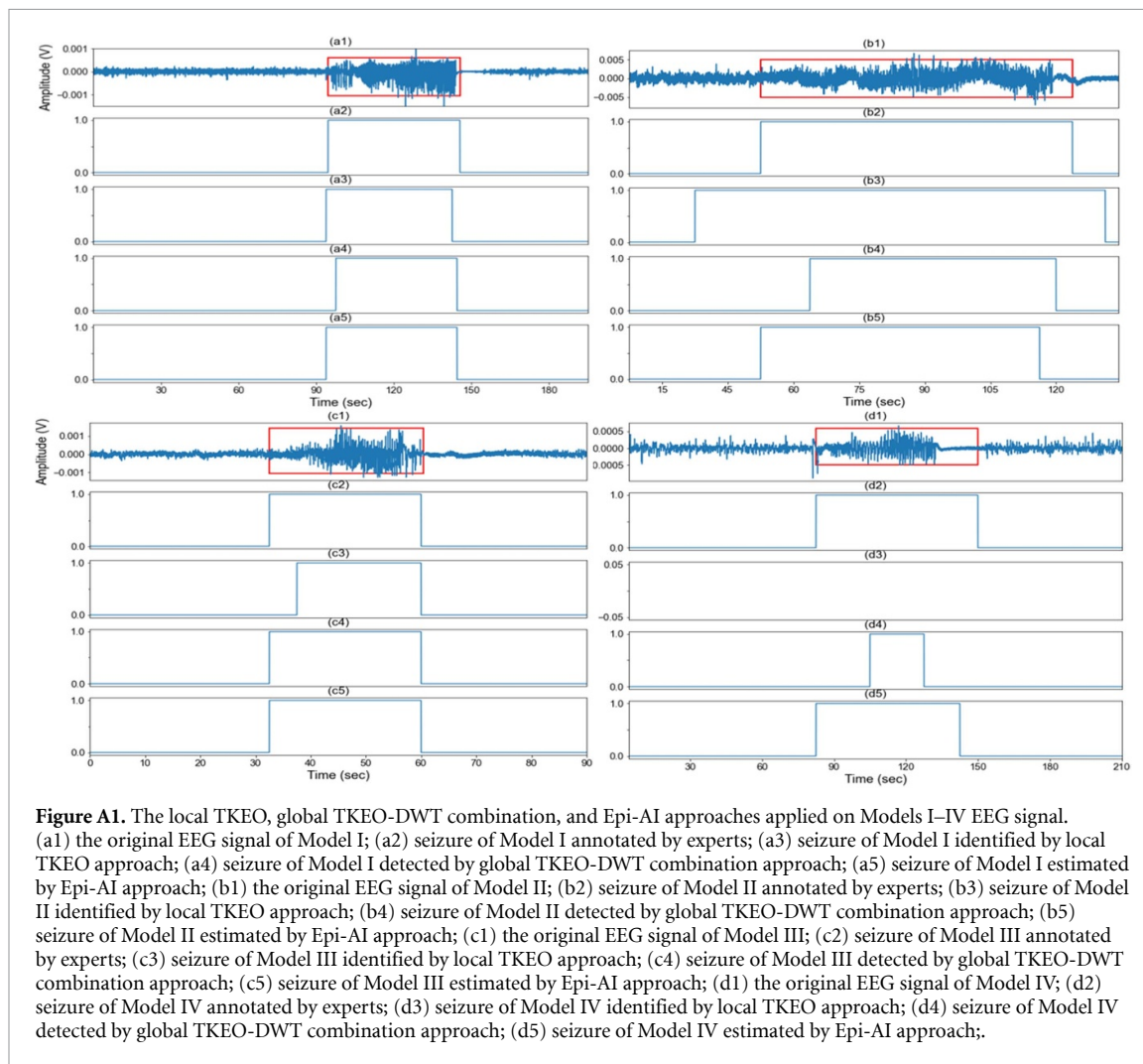| Algorithm	Acc(%)	Sens(%)	Spec(%)	AUROC
NB	01.7	99.6	01.4	0.505
KNN	99.8	01.9	99.9	0.509
DT	99.9	40.6	99.9	0.703
RF	99.9	81.2	99.9	0.906
XGboost	**97.5**	**90.4**	**97.5**	**0.939**

Figure A1. The local TKEO, global TKEO-DWT combination, and Epi-AI approaches applied on Models I–IV EEG signal. (a1) the original EEG signal of Model I; (a2) seizure of Model I annotated by experts; (a3) seizure of Model I identified by local TKEO approach; (a4) seizure of Model I detected by global TKEO-DWT combination approach; (a5) seizure of Model I estimated by Epi-AI approach; (b1) the original EEG signal of Model II; (b2) seizure of Model II annotated by experts; (b3) seizure of Model II identified by local TKEO approach; (b4) seizure of Model II detected by global TKEO-DWT combination approach; (b5) seizure of Model II estimated by Epi-AI approach; (c1) the original EEG signal of Model III; (c2) seizure of Model III annotated by experts; (c3) seizure of Model III identified by local TKEO approach; (c4) seizure of Model III detected by global TKEO-DWT combination approach; (c5) seizure of Model III estimated by Epi-AI approach; (d1) the original EEG signal of Model IV; (d2) seizure of Model IV annotated by experts; (d3) seizure of Model IV identified by local TKEO approach; (d4) seizure of Model IV detected by global TKEO-DWT combination approach; (d5) seizure of Model IV estimated by Epi-AI approach;.

ORCID iDs

Federico Del Gallo ⬤ https://orcid.org/0000-0003-0248-2456
Catherine Mooney ⬤ https://orcid.org/0000-0002-7696-1364

References

[1] Ngugi A K, Bottomley C, Kleinschmidt I, Sander J W and Newton C R 2010 Estimation of the burden of active and life-time epilepsy: a meta-analytic approach *Epilepsia* **51** 883–90

[2] Löscher W, Klitgaard H, Twyman R E and Schmidt D 2013 New avenues for anti-epileptic drug discovery and development *Nat. Rev. Drug Discovery* **12** 757–76

[3] Mouri G, Jimenez-Mateos E, Engel T, Dunleavy M, Hatazaki S, Paucard A, Matsushima S, Taki W and Henshall D C 2008 Unilateral hippocampal CA3-predominant damage and short latency epileptogenesis after intra-amygdala microinjection of kainic acid in mice *Brain Res.* **1213** 140–51

[4] Jimenez-Mateos E M *et al* 2012 Silencing microRNA-134 produces neuroprotective and prolonged seizure-suppressive effects *Nat. Med.* **18** 1087–94

[5] Venø M T *et al* 2020 A systems approach delivers a functional microRNA catalog and expanded targets for seizure suppression in temporal lobe epilepsy *Proc. Natl Acad. Sci.* **117** 15977–88

[6] Brennan G P *et al* 2020 Genome-wide microRNA profiling of plasma from three different animal models identifies biomarkers of temporal lobe epilepsy *Neurobiol. Dis.* **144** 105048

[7] Catterall W A, Kalume F and Oakley J C 2010 NaV1.1 channels and epilepsy *J. Physiol.* **588** 1849–59

[8] Mistry A M, Thompson C H, Miller A R, Vanoye C G, George Jr A L and Kearney J A 2014 Strain- and age-dependent hippocampal neuron sodium currents correlate with epilepsy severity in Dravet syndrome mice *Neurobiol. Dis.* **65** 1–11

[9] Xanthopoulos P, Liu C C, Zhang J, Miller E R, Nair S, Uthman B M, Kelly K and Pardalos P M 2009 A robust spike and wave algorithm for detecting seizures in a genetic absence seizure model *2009 Annual Int. Conf. of the IEEE Engineering in Medicine and Biology Society* (IEEE) pp 2184–7

[10] Bergstrom R A, Choi J H, Manduca A, Shin H S, Worrell G A and Howe C L 2013 Automated identification of multiple seizure-related and interictal epileptiform event types in the EEG of mice *Sci. Rep.* **3** 1483

[11] Tieng Q M, Anbazhagan A, Chen M and Reutens D C 2017 Mouse epileptic seizure detection with multiple EEG features and simple thresholding technique *J. Neural Eng.* **14** 066006

[12] Aziz O, Musngi M, Park E J, Mori G and Robinovitch S N 2017 A comparison of accuracy of fall detection algorithms (threshold-based vs. machine learning) using waist-mounted tri-axial accelerometer signals from a comprehensive set of falls and non-fall trials *Med. Biol. Eng. Comput.* **55** 45–55

[13] Pan Y, Ge S S, Al Mamun A and Tang F R 2008 Detection of seizures in EEG signal using weighted locally linear embedding and SVM classifier *2008 Conf. on Cybernetics and Intelligent Systems* (IEEE) pp 358–63

[14] Jang H J and Cho K O 2019 Dual deep neural network-based classifiers to detect experimental seizures *Korean J. Physiol. Pharmacol.* **23** 131–9

[15] Li J, Leverton L K, Naganatanahalli L M and Christian-Hinman C A 2020 Seizure burden fluctuates with the female reproductive cycle in a mouse model of chronic temporal lobe epilepsy *Exp. Neurol.* **334** 113492

[16] Miller A R, Hawkins N A, McCollom C E and Kearney J A 2014 Mapping genetic modifiers of survival in a mouse model of Dravet syndrome *Genes Brain Behav.* **13** 163–72

[17] Engel T *et al* 2013 CHOP regulates the p53–MDM2 axis and is required for neuronal survival after seizures *Brain* **136** 577–92

[18] Shokouhi N and Hansen J H 2017 Teager–Kaiser energy operators for overlapped speech detection *IEEE/ACM Trans. Audio Speech Lang. Process.* **25** 1035–47

[19] Kamath C 2013 Teager energy based filter-bank cepstra in EEG classification for seizure detection using radial basis function neural network *ISRN Biomed. Eng.* **2013** 498754

[20] Roehri N, Lina J M, Mosher J C, Bartolomei F and Bénar C G 2016 Time-frequency strategies for increasing high-frequency oscillation detectability in intracerebral EEG *IEEE Trans. Biomed. Eng.* **63** 2595–606

[21] Solnik S, Rider P, Steinweg K, DeVita P and Hortobágyi T 2010 Teager–Kaiser Operator improves the accuracy of EMG onset detection independent of signal-to-noise ratio *Eur. J. Appl. Physiol.* **110** 489–98

[22] Kumar Y, Dewal M and Anand R 2014 Epileptic seizure detection using DWT based fuzzy approximate entropy and support vector machine *Neurocomputing* **133** 271–9

[23] Sharmila A and Geethanjali P 2016 DWT Based Detection of Epileptic Seizure From EEG Signals Using Naive Bayes and k-NN Classifiers *IEEE Access* **4** 7716–27

[24] Chen D, Wan S, Xiang J and Bao F S 2017 A high-performance seizure detection algorithm based on Discrete Wavelet Transform (DWT) and EEG *PLoS One* **12** e0173138

[25] Guo L, Rivero D, Seoane J A and Pazos A 2009 Classification of EEG signals using relative wavelet energy and artificial neural networks *Proc. of the First ACM/SIGEVO Summit on Genetic and Evolutionary Computation* pp 177–84

[26] Murugappan M, Rizon M, Nagarajan R, Yaacob S, Zunaidi I and Hazry D 2007 EEG feature extraction for classifying emotions using FCM and FKM *Int. J. Comput. Commun.* **1** 21–5

[27] Moffett S X, O'Malley S M, Man S, Hong D and Martin J V 2017 Dynamics of high frequency brain activity *Sci. Rep.* **7** 15758

[28] Jatupaiboon N, Pan-ngum S and Israsena P 2013 Emotion classification using minimal EEG channels and frequency bands *The 2013 10th International Joint Conference on Computer Science and Software Engineering (JCSSE)* (IEEE) pp 21–4

[29] Polychronaki G E, Ktonas P Y, Gatzonis S, Siatouni A, Asvestas P, Tsekou H, Sakas D and Nikita K 2010 Comparison of fractal dimension estimation algorithms for epileptic seizure onset detection *J. Neural Eng.* **7** 046007

[30] Duun-Henriksen J, Kjaer T W, Madsen R E, Remvig L S, Thomsen C E and Sorensen H B D 2012 Channel selection for automatic seizure detection *Clin. Neurophysiol.* **123** 84–92

[31] Anjum S M M, Käufer C, Hopfengärtner R, Waltl I, Bröer S and Löscher W 2018 Automated quantification of EEG spikes and spike clusters as a new read out in Theiler's virus mouse model of encephalitis-induced epilepsy *Epilepsy Behav.* **88** 189–204

[32] Chatterjee S 2019 Detection of focal electroencephalogram signals using higher-order moments in EMD-TKEO domain *Healthc. Technol. Lett.* **6** 64–9

[33] Kadiyala S B and Ferland R J 2017 Dissociation of spontaneous seizures and brainstem seizure thresholds in mice exposed to eight flurothyl-induced generalized seizures *Epilepsia Open* **2** 48–58

[34] Chen T and Guestrin C 2016 XGBoost: a scalable tree boosting system *Proc. of the 22nd ACM SIGKDD Int. Conf. on Knowledge Discovery and Data Mining* pp 785–94

[35] Vanabelle P, De Handschutter P, El Tahry R, Benjelloun M and Boukhebouze M 2020 Epileptic seizure detection using EEG signals and extreme gradient boosting *J. Biomed. Res.* **34** 228

[36] Wei L and Mooney C 2020 Epileptic seizure detection in clinical EEGs using an XGBoost-based method *2020 IEEE Signal Processing in Medicine and Symp. (SPMB)* (IEEE) pp 1–6

[37] Wu J, Zhou T and Li T 2020 Detecting epileptic seizures in EEG signals with complementary ensemble empirical mode decomposition and extreme gradient boosting *Entropy* **22** 140

[38] He H, Bai Y, Garcia E A and Li S 2008 ADASYN: adaptive synthetic sampling approach for imbalanced learning *2008 IEEE Int. Conf. on Neural Networks (IEEE World Congress on Computational Intelligence)* (IEEE) pp 1322–8

[39] Causa L, Held C M, Causa J, Estévez P A, Perez C A, Chamorro R, Garrido M, Algarín C and Peirano P 2010 Automated sleep-spindle detection in healthy children polysomnograms *IEEE Trans. Biomed. Eng.* **57** 2135–46

[40] Startceva S A, Lüettjohann A, Sysoev I V and van Luijtelaar G 2015 A new method for automatic marking epileptic spike-wave discharges in local field potential signals *Saratov Fall Meeting 2014: Optical Technologies in Biophysics and Medicine XVI; Laser Physics and Photonics XVI; and Computational Biophysics* **vol 9448** (Int. Society for Optics and Photonics) p 94481R

[41] Wei L, Ventura S, Mathieson S, Boylan G, Lowery M and Mooney C 2021 Spindle-AI: sleep spindle number and duration estimation in infant EEG *IEEE Trans. Biomed. Eng.* p 1

[42] Badani S, Saha S, Kumar A, Chatterjee S and Bose R 2017 Detection of epilepsy based on discrete wavelet transform and Teager-Kaiser energy operator *2017 IEEE Conf. (CALCON)* (IEEE) pp 164–7

[43] Korkalainen H *et al* 2019 Accurate deep learning-based sleep staging in a clinical population with suspected obstructive sleep apnea *IEEE J. Biomed. Health Inform.* **24** 2073–81

[44] Zhang T, Chen W and Li M 2017 AR based quadratic feature extraction in the VMD domain for the automated seizure detection of EEG using random forest classifier *Biomed. Signal Process. Control* **31** 550–9

[45] Quigg M, Sun F, Fountain N B, Jobst B C, Wong V S, Mirro E, Brown S and Spencer D C 2015 Interrater reliability in interpretation of electrocorticographic seizure detections of the responsive neurostimulator *Epilepsia* **56** 968–71

[46] Jing J *et al* 2020 Interrater reliability of experts in identifying interictal epileptiform discharges in electroencephalograms *JAMA Neurol.* **77** 49–57

[47] Stevenson N, Tapani K, Lauronen L and Vanhatalo S 2019 A dataset of neonatal EEG recordings with seizure annotations *Sci. Data* **6** 1–8

[48] Antoniadi A M, Du Y, Guendouz Y, Wei L, Mazo C, Becker B A and Mooney C 2021 Current challenges and future opportunities for XAI in machine learning-based clinical decision support systems: a systematic review *Appl. Sci.* **11** 5088